BJP British Journal of Pharmacology

DOI:10.1111/j.1476-5381.2011.01453.x
www.brjpharmacol.org

RESEARCH PAPER

Pro-oxidant effects of Ecstasy and its metabolites in mouse brain synaptosomes

Daniel José Barbosa[1], João Paulo Capela[1,2], Jorge MA Oliveira[3], Renata Silva[1], Luísa Maria Ferreira[4], Filipa Siopa[4], Paula Sério Branco[4], Eduarda Fernandes[5], José Alberto Duarte[6], Maria de Lourdes Bastos[1] and Félix Carvalho[1]

[1]REQUIMTE (Rede de Química e Tecnologia), Laboratório de Toxicologia, Departamento de Ciências Biológicas, Faculdade de Farmácia, Universidade do Porto, Porto, Portugal, [2]Faculdade de Ciências da Saúde, Universidade Fernando Pessoa, Porto, Portugal, [3]REQUIMTE, Laboratório de Farmacologia, Departamento de Ciências do Medicamento, Faculdade de Farmácia, Universidade do Porto, Porto, Portugal, [4]REQUIMTE/CQFB (Centro de Química Fina e Biotecnologia), Departamento de Química, Faculdade de Ciências e Tecnologia, Universidade Nova de Lisboa, Caparica, Portugal, [5]REQUIMTE, Laboratório de Química Analítica e Físico-Química, Departamento de Ciências Químicas, Faculdade de Farmácia, Universidade do Porto, Porto, Portugal, and [6]CIAFEL, Departamento de Biologia do Desporto, Faculdade de Desporto, Universidade do Porto, Porto, Portugal

Correspondence
Félix Carvalho and Daniel Barbosa, REQUIMTE (Rede de Química e Tecnologia), Laboratório de Toxicologia, Departamento de Ciências Biológicas, Faculdade de Farmácia, Universidade do Porto, Rua Aníbal Cunha 164, 4050-047 Porto, Portugal. E-mail: felixdc@ff.up.pt and daniel.barbosa@ff.up.pt

Keywords
3,4-methylenedioxymethamphetamine (MDMA or 'Ecstasy'); MDMA metabolites; monoamine oxidase; mitochondria; synaptosomes; oxidative stress; neurotoxicity

Received
1 February 2011
Revised
23 March 2011
Accepted
10 April 2011

BACKGROUND AND PURPOSE
3,4-Methylenedioxymethamphetamine (MDMA or 'Ecstasy') is a worldwide major drug of abuse known to elicit neurotoxic effects. The mechanisms underlying the neurotoxic effects of MDMA are not clear at present, but the metabolism of dopamine and 5-HT by monoamine oxidase (MAO), as well as the hepatic biotransformation of MDMA into pro-oxidant reactive metabolites is thought to contribute to its adverse effects.

EXPERIMENTAL APPROACH
Using mouse brain synaptosomes, we evaluated the pro-oxidant effects of MDMA and its metabolites, α-methyldopamine (α-MeDA), N-methyl-α-methyldopamine (N-Me-α-MeDA) and 5-(glutathion-*S-yl*)-α-methyldopamine [5-(GSH)-α-MeDA], as well as those of 5-HT, dopamine, L-DOPA and 3,4-dihydroxyphenylacetic acid (DOPAC).

KEY RESULTS
5-HT, dopamine, L-DOPA, DOPAC and MDMA metabolites α-MeDA, N-Me-α-MeDA and 5-(GSH)-α-MeDA, concentration- and time-dependently increased H_2O_2 production, which was significantly reduced by the antioxidants N-acetyl-L-cysteine (NAC), ascorbic acid and melatonin. From experiments with MAO inhibitors, it was observed that H_2O_2 generation induced by 5-HT was totally dependent on MAO-related metabolism, while for dopamine, it was a minor pathway. The MDMA metabolites, dopamine, L-DOPA and DOPAC concentration-dependently increased quinoproteins formation and, like 5-HT, altered the synaptosomal glutathione status. Finally, none of the compounds modified the number of polarized mitochondria in the synaptosomal preparations, and the compounds' pro-oxidant effects were unaffected by prior mitochondrial depolarization, excluding a significant role for mitochondrial-dependent mechanisms of toxicity in this experimental model.

CONCLUSIONS AND IMPLICATIONS
MDMA metabolites along with high levels of monoamine neurotransmitters can be major effectors of neurotoxicity induced by Ecstasy.

Abbreviations

BSO, buthionine sulphoximine; DMSO, dimethylsulphoxide; DOPAC, 3,4-dihydroxyphenylacetic acid; DTNB, 5,5-dithio-bis(2-nitrobenzoic acid); FCCP, carbonyl cyanide 4-(trifluoromethoxy)phenylhydrazone; GR, glutathione reductase; GSH, reduced glutathione; 5-(GSH)-α-MeDA, 5-(glutathion-*S*-yl)-α-methyldopamine; GSSG, oxidized glutathione; HBSS/glucose, HBSS with glucose; HRP, horseradish peroxidase; MDA, 3,4-methylenedioxyamphetamine; MDMA, 3,4-methylenedioxymethamphetamine, Ecstasy; α-MeDA, α-methyldopamine; mFU, milliunits of fluorescence; NAC, N-acetyl-L-cysteine; β-NADPH, β-nicotinamide adenine dinucleotide phosphate reduced form; NBT, nitro blue tetrazolium; N-Me-α-MeDA, N-methyl-α-methyldopamine; RNS, reactive nitrogen species; ROS, reactive oxygen species; TBA, thiobarbituric acid; TBARS, thiobarbituric acid reactive substances; TBS, Tris-buffered saline solution; TBS-T, Tris-buffered saline solution with Tween 20; TCA, trichloroacetic acid; TMRM, tetramethylrhodamine methyl ester

Introduction

3,4-Methylenedioxymethamphetamine (MDMA or 'Ecstasy') is a strong psychoactive and mild hallucinogenic substance, which has become a major drug of abuse worldwide, over the last three decades (Hrometz *et al.*, 2004; Capela *et al.*, 2009). MDMA consumption has received particular attention because several studies have documented its potential neurotoxicity (see Capela *et al.*, 2009). MDMA-mediated neurotoxicity in rats essentially affects 5-hydroxytryptaminergic neurons (O'Hearn *et al.*, 1988; Bai *et al.*, 2001). On the other hand, high doses of MDMA administered to mice result in both dopaminergic and 5-hydroxytryptaminergic neurotoxicity (Stone *et al.*, 1987; Cadet *et al.*, 2001; Granado *et al.*, 2008). Several factors are thought to contribute to MDMA-induced neurotoxicity, namely hyperthermia, sustained receptor stimulation, inhibition of neurotransmitter synthesis, monoamine oxidase (MAO)-related metabolism of dopamine and 5-HT, dopamine oxidation and formation of neurotoxic metabolites of MDMA (Capela *et al.*, 2009). Oxidative stress is a common outcome of these factors and has an important role in the pathogenesis of MDMA, both in peripheral organs (Ninković *et al.*, 2008; Carvalho *et al.*, 2010; Shenouda *et al.*, 2010) and in the CNS (Sanchez *et al.*, 2003; Capela *et al.*, 2007; Alves *et al.*, 2009). However, the relative contribution of each of these factors to the neurotoxicity of MDMA remains to be elucidated.

It is well known that MDMA induces an acute and rapid release of both 5-HT and dopamine from nerve endings, which may undergo oxidative deamination by MAO, leading to the formation of deleterious amounts of hydrogen peroxide (H_2O_2) (Alves *et al.*, 2007). On the other hand, several studies failed to demonstrate 5-hydroxytryptaminergic neurotoxicity when MDMA or 3,4-methylenedioxyamphetamine (MDA) were injected directly into the brain, suggesting an important role for systemic metabolism in the neurotoxicity induced by these amphetamine derivatives (Bai *et al.*, 1999; Esteban *et al.*, 2001). The hepatic metabolism of MDMA involves N-demethylation to MDA, which is also a well-known drug of abuse. MDMA and MDA are *O*-demethylenated to N-methyl-α-methyldopamine (N-Me-α-MeDA) and α-methyldopamine (α-MeDA), respectively, both of which are catechols that can undergo oxidation to the corresponding *o*-quinones (Lim and Foltz, 1988; Pizarro *et al.*, 2004). In humans, N-Me-α-MeDA is the main plasma metabolite of MDMA, while α-MeDA is the main plasma metabolite in mice (de la Torre and Farré, 2004). These *o*-quinones are highly redox active molecules that can undergo redox cycling, generating semiquinone radicals and leading to the formation of reactive oxygen species (ROS) and reactive nitrogen species (RNS) (Erives *et al.*, 2008). In addition, as the reactive *o*-quinone intermediates are electrophilic compounds, cellular damage can occur through alkylation of crucial cellular proteins and/or DNA (Capela *et al.*, 2009). In the presence of reduced glutathione (GSH), *o*-quinones may be conjugated to form a glutathionyl adduct (Hiramatsu *et al.*, 1990). This GSH conjugate remains redox active and is readily oxidized to the quinone-thioether, which can undergo further reaction with GSH and/or protein thiols (Miller *et al.*, 1997). The systemic formation of GSH conjugates of α-MeDA and N-Me-α-MeDA is followed by uptake and further metabolism in the brain, as GSH conjugates of N-Me-α-MeDA are present in the brain of rats given MDMA by s.c. injection (Jones *et al.*, 2005; Erives *et al.*, 2008). Therefore, MDMA metabolites can be major effectors of MDMA neurotoxic effects, though the mechanisms behind their toxicity remain to be clarified.

The present study used mouse brain synaptosomes as an experimental model to further clarify the mechanisms of MDMA-induced neurotoxicity. Synaptosomes are a subcellular fraction, derived from neurons, prepared from brain tissue by homogenization and function as small anucleated cells that retain neuronal vesicles and enzymes. Usually, synaptosomes have one or more mitochondria and possess extremely active ion transport systems across their membranes (Nicholls, 1993; Whittaker, 1993). Synaptosomes have been used successfully to study metabolic pathways, relationships between energy production and ion movements, neurotransmitter storage and synthesis, and mechanisms involved in neurotransmitters release, as well as oxidative damage to macromolecules and neuronal mitochondria (Nicholls, 1993; Erecinska *et al.*, 1996). Increased ROS formation in mouse brain synaptosomes proved to be a useful index of the neurotoxicity induced by MDMA (Chipana *et al.*, 2006). Also, several studies have been conducted in synaptosomes to assess the effects on neurotransmitter uptake induced by amphetamine derivatives (Kim *et al.*, 2000; Pubill *et al.*, 2005).

In the present study, the pro-oxidant effects of MDMA and its metabolites α-MeDA, N-Me-α-MeDA and 5-(glutathion-*S-yl*)-α-methyldopamine [5-(GSH)-α-MeDA], as well as those of 5-HT, dopamine, L-DOPA and 3,4-dihydroxyphenylacetic acid (DOPAC), were evaluated in mouse brain synaptosomes through the assessment of H_2O_2 production, oxidative stress biomarkers and formation of protein quinones. We also assessed the role of mitochondria and MAO metabolism in the neurotoxic process.

Methods

Animals

All procedures were designed to minimize the number of animals used and their suffering, and were approved by the Portuguese Agency for Animal Welfare (general board of Veterinary Medicine in compliance with the Institutional Guidelines and the European Convention).

Adult male Swiss CD-1 mice (Charles River, Barcelona, Spain) weighting 30–40 g were used in all experiments. Animals were maintained under a 12 h light/dark cycle, in a temperature- and humidity-controlled room and given *ad libitum* access to food and water.

Preparation of mouse brain synaptosomes

Mouse brain synaptosomes were obtained as described elsewhere (Pubill *et al*., 2005; Chipana *et al*., 2006) with minor modifications. Briefly, on the morning of each assay, after weighing and anaesthetizing (sodium thiopental, 60 mg·kg^{-1}, i.p.) the animal, the brain was rapidly removed, weighed and placed in 20 volumes of cold homogenization buffer (5 mM Tris–HCl and 320 mM sucrose, pH 7.4). The mouse brain was homogenized using a borosilicate glass homogenizing tube fitted with a motor-driven Teflon pestle (10 strokes on ice). The homogenate was centrifuged at 1000× *g*, for 10 min, at 4°C. The supernatant was recovered, its volume was measured, and 1.6 M sucrose buffer (containing 5 mM Tris–HCl, pH 7.4) was added to a final sucrose concentration of 0.8 M. Samples were then centrifuged at 16 000× *g*, for 30 min, at 4°C, which gave a myelin-rich supernatant and a pellet (P2) consisting of mitochondria (brown-coloured) covered by a layer of synaptosomes (white). The supernatant was discarded, and the synaptosome layer was separated by carefully adding 1 mL of ice-cold 320 mM sucrose buffer (pH 7.4) and gently shaking the suspension. Finally, the synaptosome fraction was diluted in HBSS/glucose. All experiments were performed at a final protein concentration of 0.1 mg·mL^{-1}, except in assessment of mitochondrial damage, in which synaptosomes were used at a final protein concentration of 0.5 mg·mL^{-1}. Protein concentration was determined using the Bio-Rad DC protein assay kit, according to the manufacturer's specifications and using BSA solutions as standards.

Assessment of H_2O_2 production

The formation of synaptosomal H_2O_2 was measured by fluorescence, using amplex red (25 μM) in the presence of 0.25 U·mL^{-1} horseradish peroxidase (HRP), as previously described (Tretter and Adam-Vizi, 2007), with some adaptations. The method is based in the fact that H_2O_2 reacts with amplex red, a colourless and non-fluorescent compound, at a stoichiometry of 1:1, in a reaction catalysed by HRP to generate the highly fluorescent product resorufin. The fluorescence intensity is proportional to the H_2O_2 generation. Resorufin exhibits a maximum of fluorescence emission at a wavelength of 587 nm and maximum excitation at 563 nm. This is a very sensitive method for low concentrations of H_2O_2 (this procedure allows detection of 5 pmol H_2O_2 in a 96-well fluorescence assay microplate) (Zhou *et al*., 1997). The synaptosomes were exposed to the drugs under study (6.25, 12.5, 25, 50, 100 and 200 μM) and fluorescence intensities of the reaction mixtures were measured at 37°C during 15 min, using a 96-well microplate in a fluorescence microplate reader (Synergy HT; Bio-Tek Instruments, VT) with a filter set for excitation and emission at 530 ± 25 and 590 ± 35 nm respectively. Each well contained 250 μL of synaptosomal suspension, 15 μL of HRP, 15 μL of amplex red and 10 μL of compound solution. The final volume in the well was fixed with HBSS/glucose to 300 μL. In the experiments conducted in the presence of MAO inhibitors (clorgyline 100 nM and deprenyl 10 nM), antioxidants (NAC 10 and 100 μM, ascorbic acid 10 and 100 μM and melatonin 0.5 and 1 mM) and FCCP (1 μM), synaptosomes were pre-incubated with these compounds in water bath, at 37°C, for 30 min. Based on the results obtained for H_2O_2 production, the effects of antioxidants and FCCP were evaluated after incubation of synaptosomes with the drugs at a fixed concentration (50 μM). The MAO inhibitors' concentrations used in this study were selected from previous studies of MAO inhibition (Youdim *et al*., 2001; Aubin *et al*., 2004). The FCCP concentration used here was selected from studies of maximal mitochondrial depolarization in neurons (Oliveira and Gonçalves, 2009) and synaptosomes (Tretter *et al*., 1998). Mean fluorescence values of each experimental condition are presented in milliunits of fluorescence [mFU (arbitrary units)] or by the slope of the reading [mFU (arbitrary units)·min^{-1}, from 10 to 15 min].

Assessment of lipid peroxidation

Lipid peroxidation was assessed by measuring malondialdehyde equivalents, using the thiobarbituric acid (TBA) assay (as TBA reactive substances – TBARS). After incubation of synaptosomes with different concentrations of compounds (6.25, 12.5, 25, 50, 100 and 200 μM) in a water bath, at 37°C, samples of 150 μL were removed at selected time points (15, 30, 60, 120 and 180 min) and 300 μL of 10% trichloroacetic acid (TCA) (w/v) were added. The mixture was allowed to incubate on ice for 30 min before centrifugation at 16 000× *g*, for 10 min, at 4°C. After centrifugation, 250 μL of the supernatant was incubated with 250 μL of TBA reagent [1% TBA (w/v) in distilled water]. The mixture was heated at 95°C, for 10 min, and allowed to cool at room temperature. The malondialdehyde levels were estimated by spectrophotometric determination (PowerWaveX; Bio-Tek Instruments) at 535 nm. The effect promoted by 100 μM of NAC against lipid peroxidation was evaluated after incubating synaptosomes with the MDMA metabolite 5-(GSH)-α-MeDA, at the concentration of 200 μM. The amount of malondialdehyde equivalents was calculated using a molar extinction coefficient of 1.56×10^5 mol·cm^{-1}, and the final result was expressed as nmol malondialdehyde Eq·mg^{-1} protein.

Assessment of protein-bound quinones (quinoproteins)

Protein-bound quinones were assessed by the NBT/glycinate colorimetric assay, as previously described (Capela *et al*., 2007), with a few adaptations. After incubation of synaptosomes with different concentrations of drugs (6.25, 12.5, 25, 50, 100 and 200 μM) in water bath, at 37°C, sample aliquots (1 mL) were collected at selected time points (20, 30 and

60 min) and centrifuged at 16 000× *g*, for 15 min, at 37°C. The supernatant was carefully discarded, and the pellet was lysed in ice-cold RIPA buffer [50 mM Tris–HCl, 150 mM NaCl, 1% Igepal CA-630 (v/v), 0.5% sodium deoxycholate (w/v) and 0.1% SDS (w/v), pH 7.4], supplemented with 0.5 mM of PMSF. The samples were vortexed and placed in the ultrasonic bath for 10 min. Subsequently, 70 µL of the lysates in RIPA buffer were added to 180 µL of 2 M sodium glycinate solution (pH 10). The protein containing solution was added to 500 µL of NBT reagent (0.24 mM NBT in 2 M sodium glycinate, pH 10). The reaction was performed for 2 h, with agitation, at room temperature, after which the absorbance of the blue-purple colour was read at 530 nm in a 96-well plate reader (PowerWaveX; Bio-Tek Instruments). Whole protein content was quantified using the Bio-Rad DC protein assay kit and BSA solutions as standards. Results are expressed as optical density arbitrary units (OD 530 nm·mg^{-1} protein).

Assessment of protein carbonylation

Protein carbonyls, an index of protein oxidation, were determined as previously described (Magalhães *et al.*, 2007), with adaptations. After incubation of synaptosomes with 200 µM of the different compounds in a water bath at 37°C, for 2 h, 2 mL sample aliquots were removed and centrifuged at 16 000× *g*, for 15 min, at 4°C. The supernatant was discarded, and the pellet was dispersed in 300 µL of phosphate buffer (50 mM KH_2PO_4 and 1 mM EDTA, pH 6.7), sonicated and again centrifuged at 10 000× *g*, for 15 min, at 4°C. Protein concentrations of all samples were determined using the Bio-Rad DC protein assay kit, and all samples were diluted down to a final protein concentration of 0.1 mg·mL^{-1}. Samples containing 20 µg of protein (200 µL) were incubated with 400 µL of 20 mM 2,4-dinitrophenylhydrazine [in 10% trifluroacetic acid (v/v)] in the presence of 200 µL of 12% SDS (w/v), for 30 min at room temperature in the dark, after which were neutralized with 300 µL of neutralization solution [18% β-mercaptoethanol (v/v) in 2 M Tris] and diluted down to a final protein concentration of 2 µg·mL^{-1}. Derivatized proteins (0.2 µg) were loaded into nitrocellulose membrane under vacuum using a slot blot apparatus. Then, after washing in Tris-buffered saline solution (TBS:10 mM Tris–HCl, 150 mM NaCl, pH 8.0), the membrane was blocked in blocking buffer [5% non-fat powdered skim milk (w/v) in TBS with 0.05% Tween 20 (v/v) (TBS-T)] overnight, at 4°C. The membrane was then incubated with primary antibody (rabbit polyclonal anti-DNP, 1:1000) for 1.5 h. After incubation with the primary antibody, membranes were rinsed two times with TBS-T and added with the secondary antibody (anti-rabbit IgG-peroxidase, 1:2000) for 1 h. Antibodies were diluted in blocking buffer. Following two washes in TBS-T, bands were visualized by treating the immunoblots with ECL Plus chemiluminescence reagents (Amersham Pharmacia Biotech), according to the supplier's instructions, and developed on high performance chemiluminescence films (Amersham Pharmacia Biotech) with Kodak Film Developer and Kodak Fixer (Sigma-Aldrich). Bands in the films were quantified using the Image J software (National Institutes of Health). Optical density results were expressed as % of control values.

Assessment of glutathione levels

The GSH and GSSG levels of the synaptosomes were determined by the DTNB-GSH reductase recycling assay as previously described (Carvalho *et al.*, 2004a), with adaptations. After exposure of the synaptosomes to the tested compounds at the concentrations of 50 and 200 µM in water bath, at 37°C, 2 mL sample aliquots were collected at selected time points (1 and 2 h) and centrifuged at 16 000× *g*, for 15 min, at 4°C. The supernatant (600 µL) was collected, and 200 µL $HClO_4$ 20% (w/v) was added. The pellet was dispersed in 250 µL of $HClO_4$ 5% (w/v) and again centrifuged at 16 000× *g*, for 5 min, at 4°C. In sample aliquots, the perchloric acid pellet was dissolved in 250 µL of NaOH 0.3 M, and the protein content was assayed by the Lowry method (Lowry *et al.*, 1951), using BSA solutions as standards. The supernatants (200 µL) were neutralized with an equimolar solution of $KHCO_3$ (0.76 M) and centrifuged at 16 000× *g*, for 5 min, at 4°C. For GSSG quantification, aliquots (200 µL) of acidic supernatant were added of 10 µL 2-vinylpyridine and shaked continuously during 1 h to block free SH groups. In 96-well plates, 100 µL of sample, standard or blank were added in triplicate and mixed with 65 µL of fresh reagent solution containing 1.3 mM 5,5-dithio-bis(2-nitrobenzoic acid) (DTNB) and 0.24 mM β-NADPH dissolved in phosphate buffer (71.5 mM Na_2HPO_4, 71.5 mM NaH_2PO_4 and 0.63 mM EDTA, pH 7.5). Plates were then incubated in a plate reader (PowerWaveX; Bio-Tek Instruments) at 30°C during 15 min prior to the addition of 40 µL of fresh GR solution per well (10 U·mL^{-1} in phosphate buffer). The stoichiometric formation of 5-thio-2-nitrobenzoic acid (TNB) was followed for 3 min at 415 nm and compared with a standard curve. GSH and GSSG standard solutions were prepared in $HClO_4$ 5% (w/v). The effect of buthionine sulphoximine (BSO) on GSH levels was evaluated after incubating synaptosomes with the drugs, at the concentration of 200 µM, for 1 h. GSH and GSSG contents were normalized to the total protein content, and the final result was expressed as nmol GSH or GSSG·mg^{-1} protein or µM GSH in the supernatant.

Assessment of mitochondrial integrity

To assess mitochondrial integrity, synaptosomes exposed to drugs, at the concentration of 200 µM, for 1 h, were subsequently incubated with 50 nM tetramethylrhodamine methyl ester (TMRM) and imaged by fluorescence microscopy as previously described (Oliveira and Gonçalves, 2009), during 2 h. The imaging system consisted of an inverted epifluorescence microscope (Eclipse TE300; Nikon, Tokyo, Japan) equipped with a 60× air objective, a monochromator (Polychrome II; TILL Photonics, Martinsried, Germany) and a CCD camera (C6790; Hamamatsu Photonics, Hamamatsu, Japan). In each experiment, synaptosomal preparations were sampled in triplicate, by placing 20 µL of the synaptosomal suspension between glass slide and coverslip and processed with the automated acquisition of 20 random fields. The number of mitochondria (TMRM-labelled puncta, as confirmed by FCCP-induced fluorescence decay) was quantified by particle analysis using custom built macros in Image J (National Institutes of Health). Results (average number of polarized mitochondria per field) are presented as % of control.

Statistical analysis

Results are presented as mean ± SD from four to six independent experiments, with synaptosomes derived from the same number of different animals. All data were analysed using parametric tests. Statistical comparisons between groups were performed with one-way ANOVA followed by the Newman–Keuls multiple comparison *post hoc* test, for experiments with one variable. Two-way ANOVA followed by the Bonferroni's multiple comparison *post hoc* test, was used in experiments with two variables. Details of the statistical analysis are described in each figure legend. Differences were considered to be statistically significant at *P*-values lower than 0.05. All analyses were performed using GraphPad Prism 5.0 for Windows (GraphPad Software, San Diego, CA).

Materials

All reagents used in this study were of analytical grade or of the highest grade available. The following reagents were obtained from Sigma-Aldrich (St. Louis, MO): N-acetyl-3,7-dihydroxyphenoxazine (amplex red), horseradish peroxidase (HRP), 5-HT hydrochloride, dopamine hydrochloride, L-DOPA, DOPAC, *R*-(–)-deprenyl hydrochloride, N-methyl-*N*-propargyl-3-(2,4-dichlorophenoxy)propylamine hydrochloride (clorgyline), N-acetyl-l-cysteine (NAC), ascorbic acid, melatonin, carbonyl cyanide 4-(trifluoromethoxy)phenylhydrazone (FCCP), thiobarbituric acid (TBA), PMSF, nitro blue tetrazolium (NBT), sodium glycinate, GSH, oxidized glutathione (GSSG), β-NADPH, 5,5-dithio-bis(2-nitrobenzoic acid) (DTNB), glutathione reductase (GR), buthionine sulphoximine (BSO) and bovine serum albumin (BSA). Rabbit polyclonal anti-DNP antibody and tetramethylrhodamine methyl ester (TMRM) were obtained from Invitrogen (Carlsbad, CA). Anti-rabbit IgG-peroxidase antibody was purchased from Amersham Pharmacia Biotech (Buckinghamshine, United Kingdom). Bio-Rad DC protein assay kit was purchased from Bio-Rad Laboratories (Hercules, CA). $HClO_4$, NaOH, absolute ethanol, dimethylsulphoxide (DMSO) and Folin reagent were obtained from Merck (Darmstadt, Germany). Sodium thiopental was obtained from B. Braun (Lisbon, Portugal). MDMA (hydrochloride salt) was extracted and purified from high-purity MDMA tablets that were kindly provided by the Portuguese Criminal Police Department. The obtained salt was pure and fully characterized by NMR and mass spectrometry methodologies. The MDMA metabolites α-MeDA, N-Me-α-MeDA and 5-(GSH)-α-MeDA were synthesized and fully characterized by NMR and mass spectrometry methodologies by REQUIMTE/CQFB (Centro de Química Fina e Biotecnologia), Departamento de Química, Faculdade de Ciências e Tecnologia, Universidade Nova de Lisboa, according to methods previously published by our group (Capela *et al.*, 2006; Macedo *et al.*, 2007). All other chemicals were purchased from Sigma-Aldrich. 5-HT, dopamine, DOPAC, MAO inhibitors clorgyline and deprenyl, NAC and ascorbic acid were dissolved in HEPES-buffered salt solution with glucose (HBSS/glucose: 140 mM NaCl, 5.37 mM KCl, 1.26 mM $CaCl_2$, 0.44 mM KH_2PO_4, 0.49 mM $MgCl_2{\cdot}6H_2O$, 0.41 mM $MgSO_4$(7H_2O, 4.17 mM $NaHCO_3$, 0.34 mM $Na_2HPO_4{\cdot}7H_2O$, 20 mM HEPES-Na and 5.5 mM glucose, pH 7.4). HRP, BSO, MDMA and MDMA metabolites were dissolved in distilled water. L-DOPA was solubilized in 10 mM HCl. Amplex red and TMRM were dissolved in DMSO. PMSF and melatonin were solubilized in absolute ethanol. FCCP was dissolved in 95% of ethanol. Controls received an equivalent amount of vehicle.

Results

MDMA metabolites, monoamine neurotransmitters, L-DOPA and DOPAC induced H_2O_2 generation in a concentration- and time-dependent manner

Mouse brain synaptosomes were exposed to growing concentrations of the different compounds (6.25–200 μM) and assayed for H_2O_2 generation, using an amplex red method. Incubation of synaptosomes with MDMA metabolites α-MeDA, N-Me-α-MeDA and 5-(GSH)-α-MeDA, as well as 5-HT, dopamine, L-DOPA and DOPAC significantly increased H_2O_2 production (Figure 1) in a concentration- and time-dependent manner. On the other hand, MDMA did not significantly increase the H_2O_2 formation at any of the evaluated concentrations during the time course of the experiment (Figure 1A). For N-Me-α-MeDA, 5-HT, L-DOPA and DOPAC, there was a statistically significant amount of H_2O_2 at the lowest concentration studied (6.25 μM) (Figure 1C,E,G,H). The other compounds generated a significant amount of H_2O_2 only at 12.5 μM or above (Figure 1B,D,F). The MDMA metabolite 5-(GSH)-α-MeDA was the most effective generator of H_2O_2, under our conditions. In experiments conducted in the absence of amplex red, no auto-fluorescence was observed for all studied compounds (data not shown).

DA- and 5-HT-induced H_2O_2 production was dependent on MAO-related metabolism

Figure 2 presents the results for H_2O_2 production, expressed by the slope of the reading [mFU (arbitrary units)·min^{-1}, from 10 to 15 min], when synaptosomes were pre-incubated with MAO-A and/or MAO-B selective inhibitors clorgyline (100 nM) and deprenyl (10 nM), respectively. There were no significant differences in basal H_2O_2 production between synaptosomes pre-incubated with MAO inhibitor(s) and non pre-incubated synaptosomes. Pre-incubation of synaptosomes with clorgyline blocked H_2O_2 production for all concentrations of 5-HT tested (Figure 2A). However, for dopamine (Figure 2B), clorgyline decreased H_2O_2 generation only at the highest dopamine concentration tested (200 μM) ($P < 0.001$), with similar effects for deprenyl ($P < 0.05$) (Figure 2B). On the other hand, MAO-B inhibition with deprenyl did not affect H_2O_2 generation by 5-HT (Figure 2A). In another set of experiments, the results of pre-incubation with clorgyline and deprenyl were similar to those obtained with clorgyline alone (Figure 2C–D). For the other compounds, pretreatment of synaptosomes with MAO inhibitors had no effect on H_2O_2 production (data not shown).

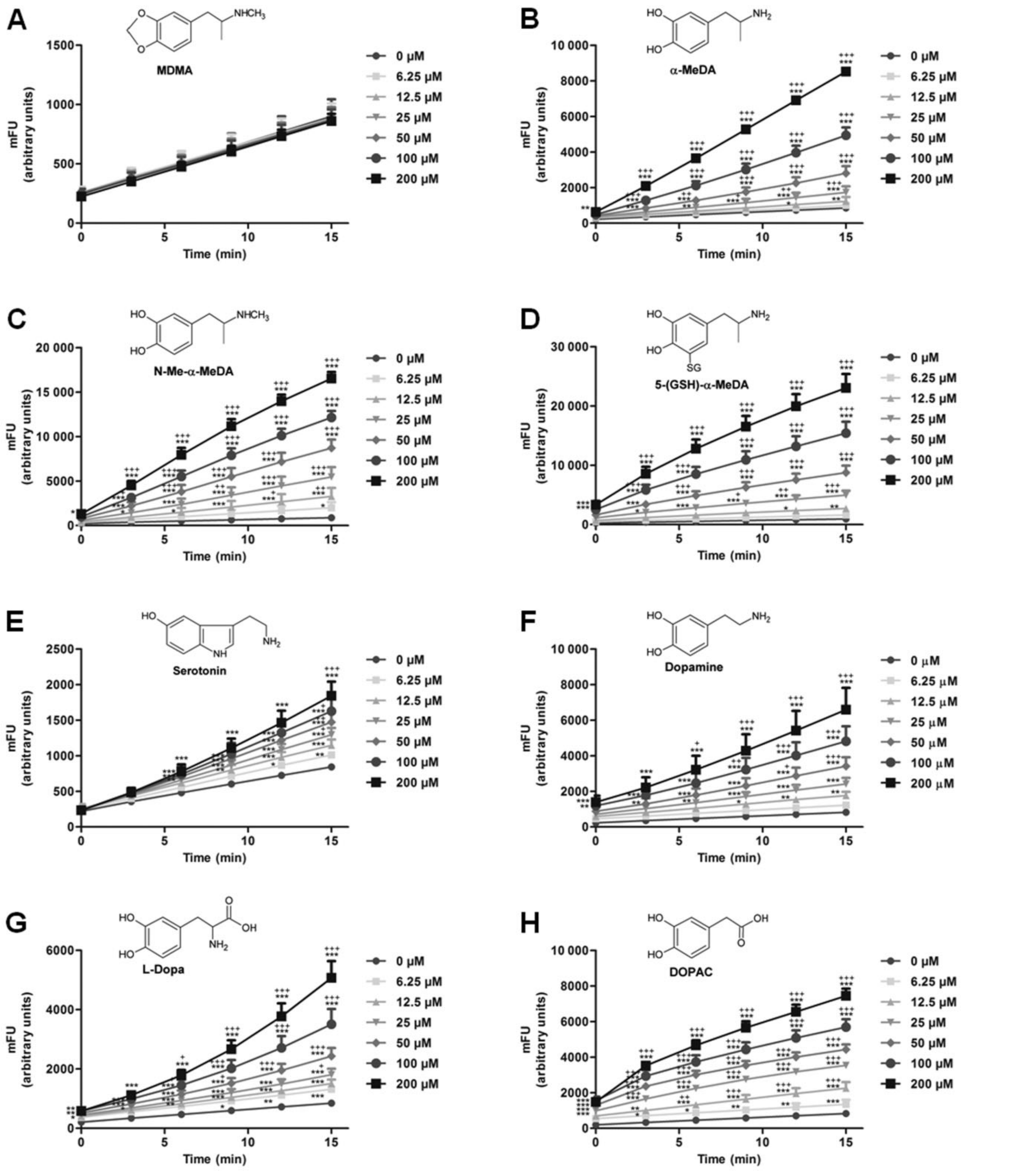

Figure 1

H_2O_2 generation induced by MDMA (A), its metabolites α-MeDA (B), N-Me-α-MeDA (C) and 5-(GSH)-α-MeDA (D), monoamine neurotransmitters 5-HT (E) and dopamine (F), as well as the dopamine precursor L-DOPA (G) and dopamine metabolite DOPAC (H), in mouse brain synaptosomes, evaluated by the amplex red method. Synaptosomes were exposed, for 15 min, to increasing concentrations (6.25, 12.5, 25, 50, 100 and 200 μM) of the compounds, and measurements were made at six different time points. Results are presented as mean ± SD from 5 independent experiments for panel A and 6 independent experiments for panels B–H, expressed in mFU (arbitrary units). Statistical comparisons were made using two-way ANOVA with repeated measures followed by the Bonferroni's multiple comparison *post hoc* test [$^{*}P < 0.05$, $^{**}P < 0.01$, $^{***}P < 0.001$ concentration vs. control (0 μM); $^{+}P < 0.05$, $^{++}P < 0.01$, $^{+++}P < 0.001$ concentration vs. prior concentration].

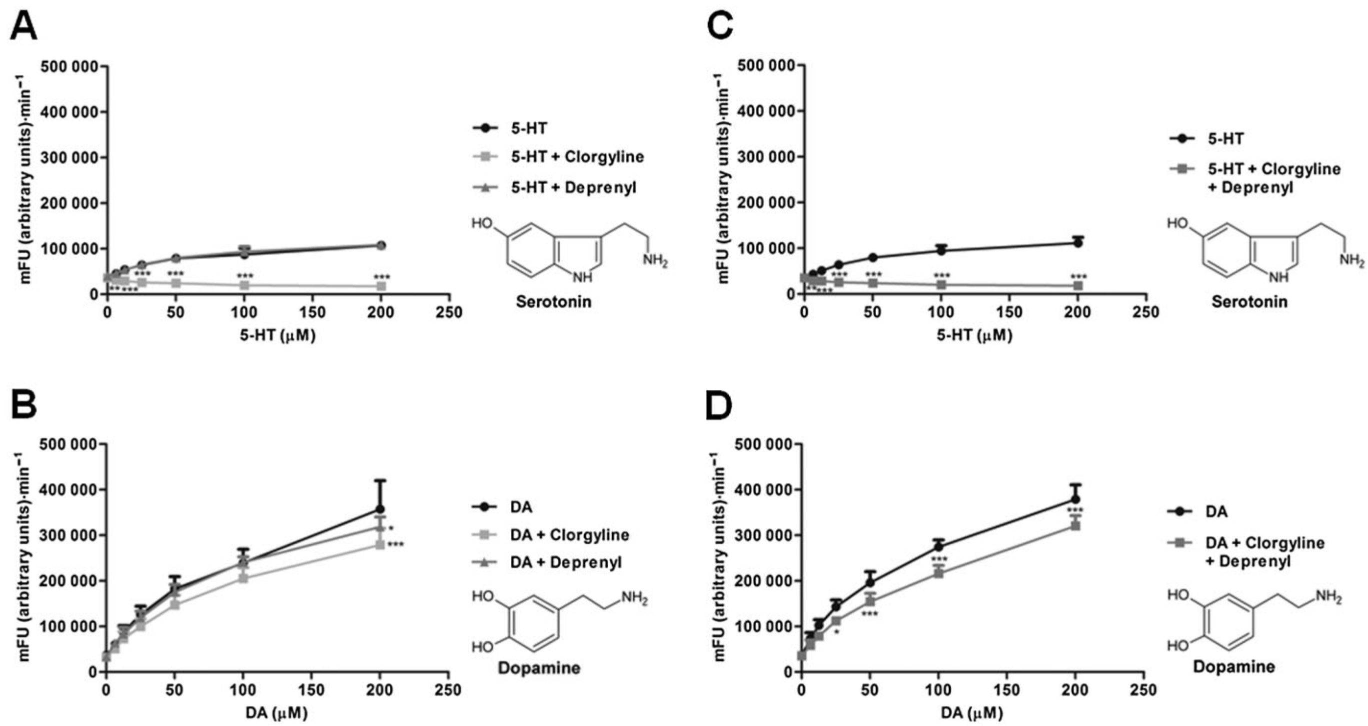

Figure 2

Effect of clorgyline (MAO-A inhibitor) or deprenyl (MAO-B inhibitor) on H_2O_2 generation induced by 5-HT and dopamine, in mouse brain synaptosomes, evaluated by the amplex red method. Synaptosomes were exposed, for 15 min, to increasing concentrations (6.25, 12.5, 25, 50, 100 and 200 μM) of 5-HT (A) or dopamine (B) either with or without clorgyline (100 nM) or deprenyl (10 nM) pre-incubation. On another set of experiments, synaptosomes were pre-incubated with clorgyline (100 nM) plus deprenyl (10 nM) before exposure to 5-HT (C) and dopamine (D). Results are presented as mean ± SD from 6 independent experiments, expressed by the slope of the reading [mFU (arbitrary units)·min^{-1}, from 10 to 15 min]. Statistical comparisons were made using two-way ANOVA followed by the Bonferroni's multiple comparison *post hoc* test [**P* < 0.05, ***P* < 0.01, ****P* < 0.001 monoamine plus MAO inhibitor(s) vs. monoamine].

NAC, ascorbic acid and melatonin prevented H_2O_2 generation induced by MDMA metabolites, 5-HT, dopamine, L-DOPA and DOPAC

Figure 3 shows the antioxidant effects of 10 μM NAC, 10 μM ascorbic acid and 0.5 mM melatonin, on H_2O_2 production. Ascorbic acid, by itself, increased H_2O_2 generation. For the MDMA metabolite α-MeDA, (Figure 3A), NAC (P < 0.05), ascorbic acid (P < 0.001) and melatonin (P < 0.001) decreased H_2O_2 production. Ascorbic acid decreased H_2O_2 production by N-Me-α-MeDA (Figure 3B) more effectively. On the other hand, for the MDMA metabolite 5-(GSH)-α-MeDA (Figure 3C) and 5-HT (Figure 3D), only melatonin decreased H_2O_2 levels (P < 0.001). Both ascorbic acid and melatonin decreased (P < 0.001) H_2O_2 levels generated by dopamine (Figure 3E). All three antioxidants decreased H_2O_2 levels resulting from incubation with L-DOPA (P < 0.001 for all antioxidants) (Figure 3F). In contrast with all other studied compounds, for DOPAC (Figure 3G), only ascorbic acid was able to decrease H_2O_2 levels (P < 0.001) but with NAC, there was actually an abrupt increase. When higher concentrations (100 μM) of the antioxidants were tested, only NAC and ascorbic acid inhibited H_2O_2 production induced by N-Me-α-MeDA (P < 0.001), while in the case of L-DOPA, only 100 μM of NAC significantly decreased H_2O_2 levels (P < 0.001) (data not shown). Also, the effects elicited by a higher concentration of melatonin (1 mM) were not significantly different from 0.5 mM for all compounds tested (data not shown). Thus, among the antioxidants studied, melatonin showed the highest antioxidant effects against H_2O_2 production induced by the different compounds.

H_2O_2 production induced by the tested compounds was unaffected by prior mitochondrial depolarization

To investigate if H_2O_2 production induced by the different compounds had a mitochondrial source, we used the protonophore FCCP that depolarizes mitochondria by collapsing the proton gradient across the mitochondrial inner membrane and dissipating mitochondrial membrane potential. Table 1 shows that FCCP (1 μM) did not affect either the basal H_2O_2 production or that induced by any of the evaluated compounds. In experiments conducted by real-time fluorescence videomicroscopy, we confirmed that the FCCP concentration used in this study was able to completely collapse the mitochondrial membrane potential (data not shown). Thus, in our experimental conditions, the H_2O_2 production induced by all tested compounds was independent of the mitochondrial polarization status,

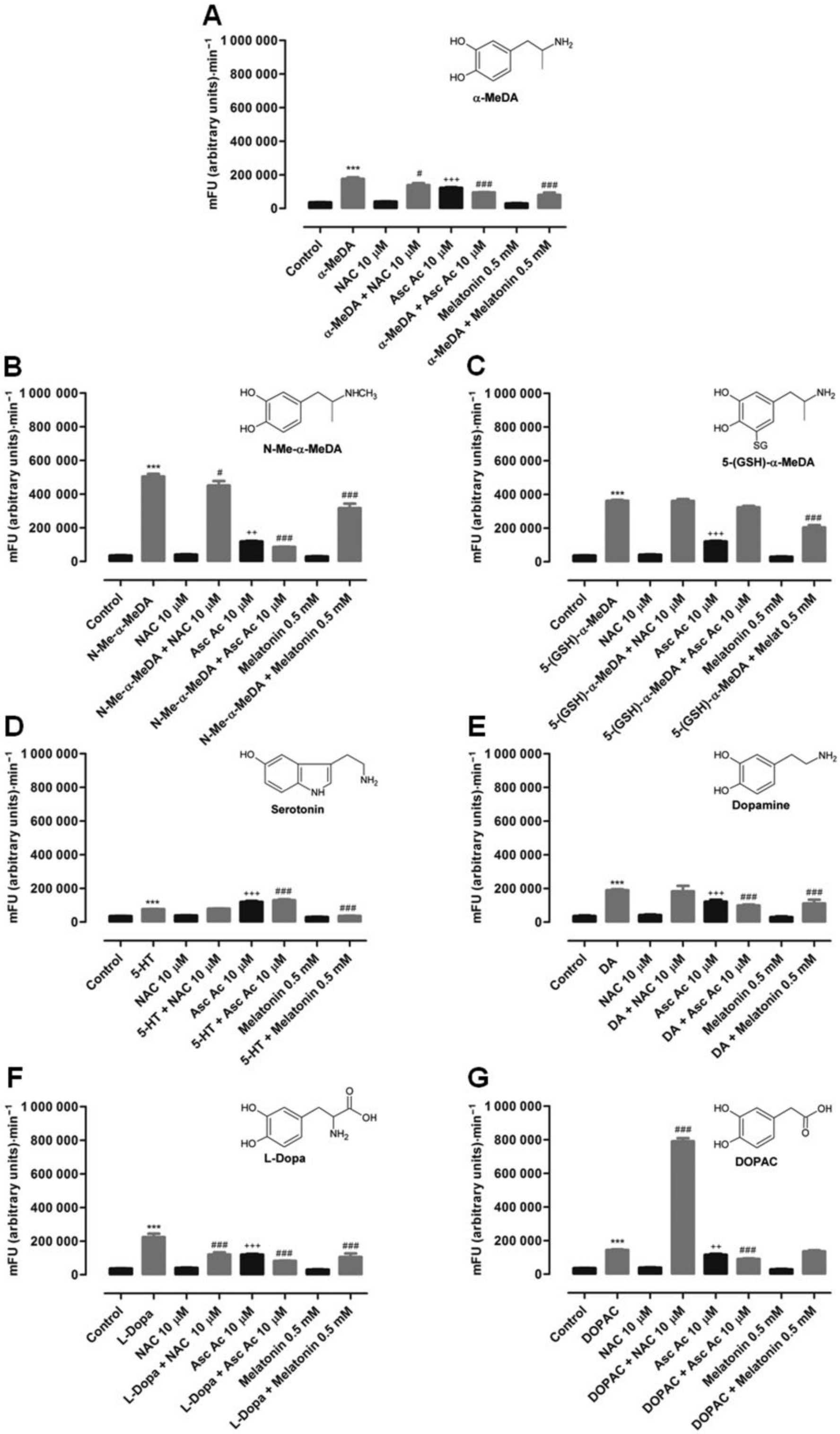

Figure 3

Protective effect of NAC, ascorbic acid and melatonin against H_2O_2 generation induced by the MDMA metabolites α-MeDA (A), N-Me-α-MeDA (B) and 5-(GSH)-α-MeDA (C), 5-HT (D), dopamine (E), L-DOPA (F) and DOPAC (G) in mouse brain synaptosomes, evaluated by the amplex red method. Synaptosomes, with or without antioxidant pre-incubation (10 μM of NAC and ascorbic acid or 0.5 mM of melatonin), were exposed for 15 min to the compounds, at the concentration of 50 μM. Results are presented as mean ± SD from 6 independent experiments, expressed by the slope of the reading [mFU (arbitrary units)·min^{-1}, from 10 to 15 min]. Statistical comparisons were made using one-way ANOVA followed by the Newman–Keuls multiple comparison *post hoc* test (****P* < 0.001 compound vs. control; $^{++}P < 0.01$, $^{+++}P < 0.001$ antioxidant vs. control; $^{\#}P < 0.05$, $^{\#\#\#}P < 0.001$ compound plus antioxidant vs. compound).

Table 1

Effect of mitochondrial depolarization with FCCP (1 μM) on H_2O_2 generation induced by MDMA metabolites, as well as by 5-HT, dopamine, L-DOPA and DOPAC

Compound	Control	FCCP 1 μM	50 μM	50 μM + FCCP 1 μM
α-MeDA	3.97 ± 0.16	4.06 ± 0.20	9.96 ± 2.06	10.85 ± 1.92
N-Me-α-MeDA	3.99 ± 0.15	4.04 ± 0.17	13.69 ± 3.49	16.83 ± 4.18×
5-(GSH)-α-MeDA	4.17 ± 0.38	4.14 ± 0.36	10.82 ± 2.29	11.54 ± 2.16
5-HT	3.85 ± 0.16	3.98 ± 0.22	7.39 ± 0.48	7.32 ± 0.52
DA	3.88 ± 0.16	3.96 ± 0.20	18.28 ± 2.09	18.17 ± 1.85
L-DOPA	3.96 ± 0.20	4.04 ± 0.23	8.50 ± 1.57	9.62 ± 1.84
DOPAC	3.86 ± 0.25	3.95 ± 0.25	15.32 ± 1.40	15.88 ± 1.49

Synaptosomes, with or without FCCP (1 μM) pretreatment were exposed for 15 min to MDMA metabolites (α-MeDA, N-Me- α-MeDA and 5-(GSH)-α-MeDA), 5-HT, dopamine, L-DOPA or DOPAC, all at 50 μM, and H_2O_2 generation was evaluated by the amplex red method. Results are presented as mean ± SD from 6 independent experiments, expressed by the slope of the reading [10^4mFU (arbitrary units)·min^{-1}, from 10 to 15 min]. Statistical comparisons were made using one-way ANOVA followed by the Newman–Keuls multiple comparison *post hoc* test.

excluding a significant role of the organelle's respiratory chain in the H_2O_2-generating mechanism.

MDMA metabolite 5-(GSH)-α-MeDA concentration- and time-dependently induced lipid peroxidation, an effect prevented by NAC

Lipid peroxidation induced by the compounds in mouse brain synaptosomes was evaluated by the TBA assay. As shown in Figure 4, the MDMA metabolite 5-(GSH)-α-MeDA induced lipid peroxidation in a concentration- and time-dependent manner, reaching significance at 120 min (Figure 4A). For the remaining compounds, we did not observe significant differences from control at any of concentrations and incubation times studied (data not shown). Experiments were conducted to verify the ability of this metabolite to react directly with the TBA. After exposure of the MDMA metabolite directly with TBA in HBSS/glucose, we verified the absence of any reaction, excluding also the possibility of reaction with the final products of the lipid peroxidation (data not shown).

Pre-incubation of synaptosomes with NAC (100 μM), inhibited lipid peroxidation mediated by 5-(GSH)-α-MeDA (200 μM) (Figure 4B). Other antioxidant treatments (NAC 10 μM, ascorbic acid 10 and 100 μM, or melatonin 0.5 and 1 mM) did not change lipid peroxidation induced by 5-(GSH)-α-MeDA (data not shown).

MDMA metabolites α-MeDA, N-Me-α-MeDA and 5-(GSH)-α-MeDA, as well as dopamine, L-DOPA and DOPAC increased the formation of protein-bound quinones, in a concentration-dependent manner

To assess the role of quinones in the deleterious potential of the different studied compounds, we evaluated the levels of protein-bound quinones (quinoproteins). Although different incubation times were tested (20, 30 and 60 min), formation of protein-bound quinones was not time-dependent, and, thus, only the results obtained at 30 min time point are presented (Figure 5). MDMA and 5-HT did not generate quinoproteins, at any of the concentrations studied (data not shown). The other compounds increased quinoprotein levels, in a concentration-dependent manner (Figure 5), and the most effective was the MDMA metabolite N-Me-α-MeDA, with a significant formation of quinoproteins at the lowest concentration studied (6.25 μM) ($P < 0.05$) (Figure 5B). The antioxidants NAC (10 and 100 μM), ascorbic acid (10 and 100 μM) and melatonin (0.5 and 1 mM) did not prevent the formation of quinoproteins (data not shown).

The MDMA metabolite 5-(GSH)-α-MeDA and DOPAC induced a significant carbonylation of synaptosomal proteins

To evaluate possible oxidative effects to synaptosomal proteins, we also studied the protein carbonylation by an immunoblotting method. As presented in Figure 6, the levels of protein carbonyls in the synaptosomes were raised by incubation with the MDMA metabolite 5-(GSH)-α-MeDA or DOPAC (200 μM), for 2 h ($P < 0.05$) but not by the other compounds (data not shown).

Incubation of synaptosomes with MDMA metabolites α-MeDA, N-Me-α-MeDA and 5-(GSH)-α-MeDA, as well as 5-HT, dopamine, L-DOPA and DOPAC altered the intra-synaptosomal glutathione status

Figure 7 shows the glutathione status in synaptosomes after incubation with 50 and 200 μM of the tested compounds for 1 and 2 h. Incubation of synaptosomes, for 1 h, with 50 μM of MDMA metabolites α-MeDA, N-Me-α-MeDA and 5-(GSH)-α-MeDA and dopamine increased total GSH levels ($P < 0.001$, $P < 0.01$, $P < 0.01$ and $P < 0.01$ respectively) (Figure 7A), without affecting GSSG levels (Figure 7E). After 2 h, there was also a significant increase in total GSH levels, only for the MDMA metabolite α-MeDA and dopamine ($P < 0.01$) (Figure 7B), without changing GSSG levels (Figure 7F).

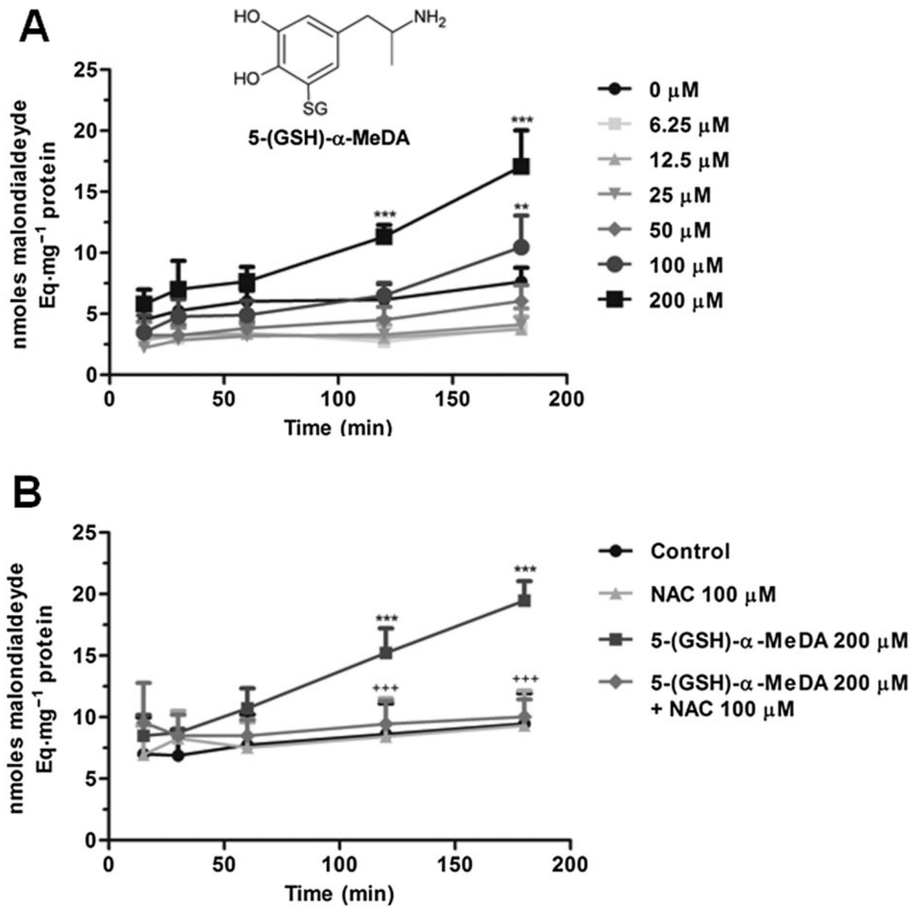

Figure 4

(A) Lipid peroxidation induced by the MDMA metabolite 5-(GSH)-α-MeDA in mouse brain synaptosomes, evaluated by the TBA assay (TBARS). Synaptosomes were exposed, for 3 h, to increasing concentrations (6.25, 12.5, 25, 50, 100 and 200 μM) of MDMA metabolite 5-(GSH)-α-MeDA, and measurements were made at 5 different time-points (15, 30, 60, 120 and 180 min). (B) Protective effect of NAC against lipid peroxidation induced by the MDMA metabolite 5-(GSH)-α-MeDA, in mouse brain synaptosomes, evaluated by the TBA assay (TBARS). Synaptosomes were exposed for 3 h to MDMA metabolite 5-(GSH)-α-MeDA, at the concentration of 200 μM, in the presence or absence of NAC (100 μM). Results are presented as mean ± SD from $n = 6$ independent experiments, expressed in nmol malondialdehyde Eq·mg^{-1} protein. Statistical comparisons were made using two-way ANOVA followed by the Bonferroni's multiple comparison *post hoc* test [$^{**}P < 0.01$, $^{***}P < 0.001$ concentration vs. control (0 μM); $^{+++}P < 0.001$ 5-(GSH)-α-MeDA plus NAC vs. 5-(GSH)-α-MeDA].

However, for the MDMA metabolite 5-(GSH)-α-MeDA, GSSG levels were significantly increased at this time point ($P < 0.05$) (Figure 7F). When synaptosomes were incubated with 200 μM of the different compounds, for 1 h, it was observed a significant increase in total GSH levels for all compounds, except for MDMA and DOPAC ($P < 0.05$ for α-MeDA, N-Me-α-MeDA, 5-(GSH)-α-MeDA, 5-HT and dopamine, and $P < 0.01$ for L-DOPA) (Figure 7C). For N-Me-α-MeDA, 5-(GSH)-α-MeDA and dopamine, the increase in total GSH levels were accompanied by significant elevations of GSSG levels ($P < 0.01$, $P < 0.001$ and $P < 0.001$, respectively) (Figure 7G). Incubation of synaptosomes with the different compounds at a concentration of 200 μM, for 2 h, resulted in significant increases in total GSH levels only after exposure to 5-HT ($P < 0.05$) and L-DOPA ($P < 0.001$) (Figure 7D), which were accompanied by increased GSSG levels ($P < 0.001$ and $P < 0.01$ respectively) (Figure 7H). At the same time point, 200 μM N-Me-α-MeDA, 5-(GSH)-α-MeDA, dopamine and DOPAC also promoted a significant increase in GSSG levels ($P < 0.01$, $P < 0.001$, $P < 0.001$ and $P < 0.01$, respectively) (Figure 7H).

In order to explain the increase of total GSH levels without concomitant elevations in the GSSG levels, we used BSO, a selective and potent inhibitor of γ-glutamylcysteine ligase (the enzyme catalysing the rate limiting step in GSH biosynthesis), and measured total GSH levels in the incubation medium after incubation with the different compounds (200 μM; 1 h). Pre-incubation of synaptosomes with BSO (Figure 8A) did not modify the basal GSH content of synaptosomes or that after incubation with the compounds. However, in the supernatant, total GSH levels decreased ($P < 0.05$ for N-Me-α-MeDA, $P < 0.01$ for 5-HT and L-DOPA and $P < 0.001$ for α-MeDA, 5-(GSH)-α-MeDA, dopamine and DOPAC) (Figure 8B), but GSSG levels remained below the detection limit of the method. Thus, the increase in total GSH levels observed did not result from an increase in its synthesis, as ascertained by the use of BSO, but rather to the uptake from the incubation medium.

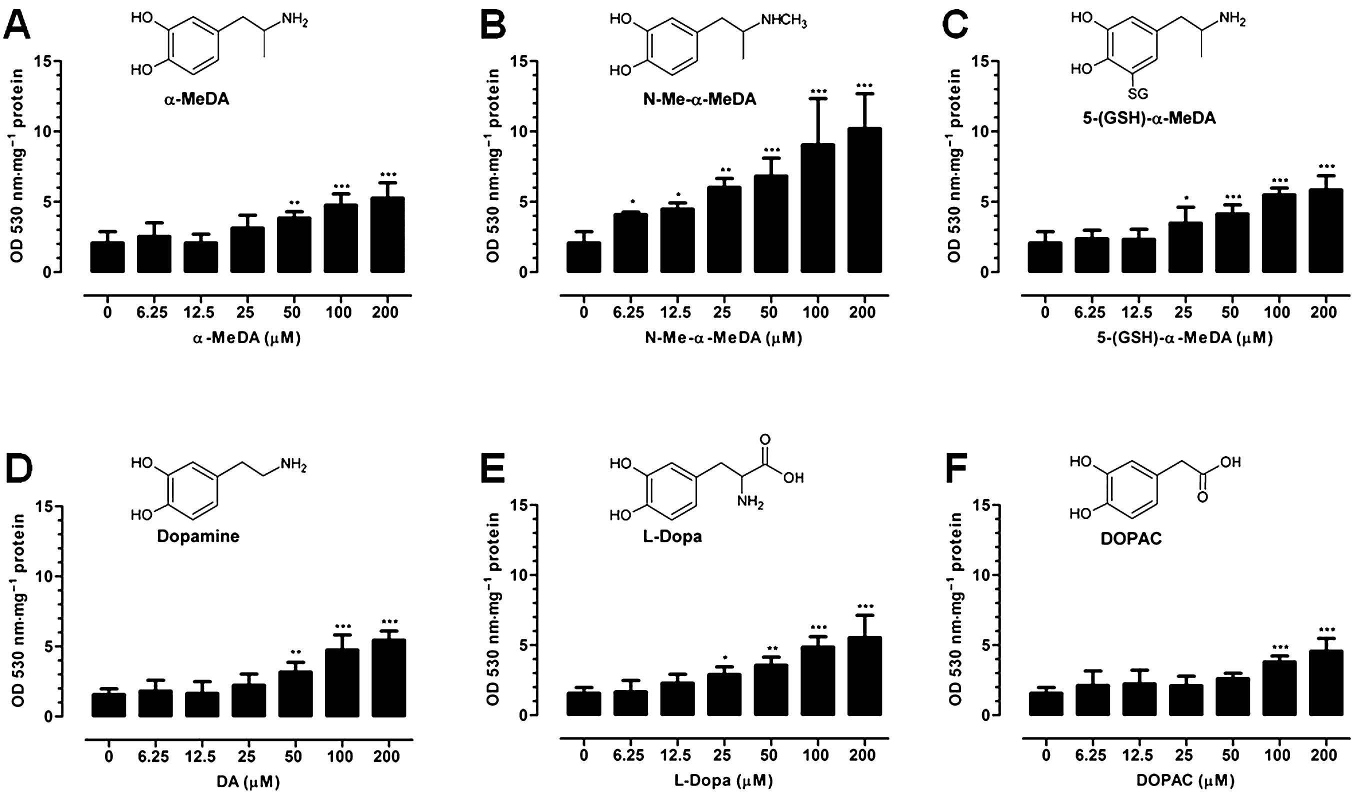

Figure 5

Protein-bound quinones (quinoproteins) induced by the MDMA metabolites α-MeDA (A), N-Me-α-MeDA (B) and 5-(GSH)-α-MeDA (C), as well as by dopamine (D), L-DOPA (E) and DOPAC (F), in mouse brain synaptosomes, evaluated by the NBT/glycinate colorimetric assay. Synaptosomes were exposed to increasing concentrations of the compounds (6.25, 12.5, 25, 50, 100 and 200 μM), and measurements were made after 30 min. Results are presented as mean ± SD from 6 independent experiments, expressed as OD 530 nm·mg^{-1} protein. Statistical comparisons were made using one-way ANOVA followed by the Newman–Keuls multiple comparison *post hoc* test [*$P < 0.05$, **$P < 0.01$, ***$P < 0.001$ concentration vs. control (0 μM)].

Oxidative stress induced by MDMA metabolites N-Me-α-MeDA and 5-(GSH)-α-MeDA and 5-HT did not alter the number of polarized mitochondria

To evaluate possible effects of 5-HT, N-Me-α-MeDA and 5-(GSH)-α-MeDA on mitochondrial integrity, we quantified the number of polarized mitochondria labelled with TMRM (50 nM). Representative images of the synaptosomes and their mitochondria are depicted in Figure 9A (bright field) and Figure 9B (TMRM fluorescence). As shown in Figure 9C, the number of polarized mitochondria after incubation of the synaptosomes, for 1 h, with 200 μM of 5-HT, N-Me-α-MeDA or 5-(GSH)-α-MeDA, was not different from the controls.

Discussion

Key findings of our study in synaptosomes were as follows: (i) MDMA metabolites α-MeDA, N-Me-α-MeDA and 5-(GSH)-α-MeDA, as well as 5-HT, dopamine, L-DOPA and DOPAC induced extensive H_2O_2 generation, in a concentration- and time-dependent manner; (ii) H_2O_2 production induced by 5-HT was fully dependent on MAO-A metabolism, while for dopamine, it was partly dependent on both MAO-A and MAO-B; (iii) NAC, ascorbic acid and melatonin decreased H_2O_2 levels in synaptosomes exposed to MDMA metabolites, as well as 5-HT, dopamine, L-DOPA and DOPAC; (iv) H_2O_2 production promoted by the tested compounds was independent of mitochondrial polarization status; (v) the MDMA metabolite 5-(GSH)-α-MeDA induced lipid peroxidation in a concentration- and time-dependent manner, an effect prevented by NAC; (vi) formation of protein-bound quinones (quinoproteins) induced by the studied compounds, except MDMA and 5-HT, was concentration-dependent but time-independent; (vii) MDMA metabolite 5-(GSH)-α-MeDA and DOPAC induced protein carbonylation; (viii) all studied compounds, except MDMA, altered the synaptosomal glutathione status; and (ix) MDMA metabolites presented a higher toxic potential than the parent compound MDMA, with 5-(GSH)-α-MeDA promoting higher oxidative stress.

Although MDMA is known to promote brain oxidative stress in laboratory animals (Alves *et al.*, 2007; 2009; Granado *et al.*, 2008), the underlying mechanisms remain largely unknown. MDMA metabolites can be major contributors (Capela *et al.*, 2006; 2007), and there is a role for dopamine

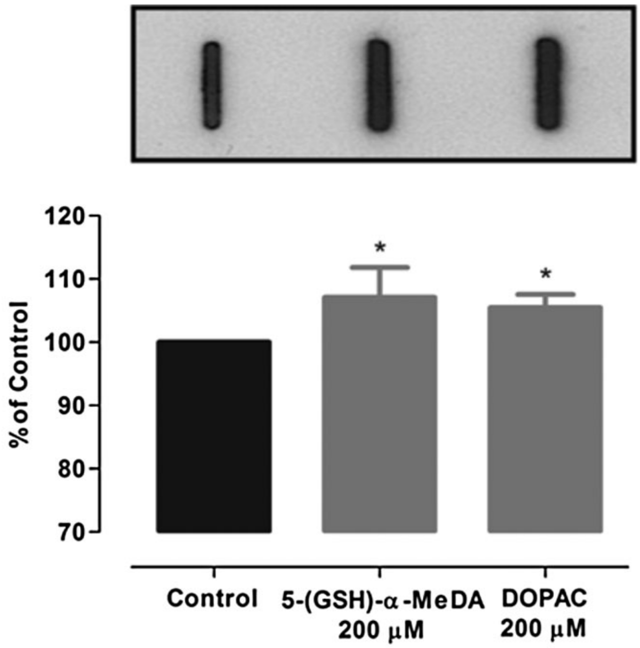

Figure 6

Protein carbonylation induced by 200 μM of the MDMA metabolite 5-(GSH)-α-MeDA and DOPAC, after exposure of synaptosomes for 2 h, evaluated by an immunoblotting method. Results are presented as mean ± SD from 4 independent experiments, expressed in percentage of control, which values were set to 100%. Statistical comparisons were made using one-way ANOVA followed by the Newman–Keuls multiple comparison *post hoc* test (*$P < 0.05$ compound vs. control).

and 5-HT in MDMA-induced neurotoxicity (Hrometz *et al.*, 2004). We found that the monoamine neurotransmitters 5-HT and dopamine, as well as the dopamine precursor (L-DOPA) and its metabolite (DOPAC), increased H_2O_2 production (Figure 1E–H).

After MDMA administration to experimental animals, there is an abrupt increase in the extravesicular levels of monoamine neurotransmitters inside nerve endings, which are metabolized by MAO (Alves *et al.*, 2007) and a byproduct of MAO action is H_2O_2, which subsequently may be converted into the hydroxyl radical, a highly cytotoxic ROS (Nagatsu, 2004). In mouse brain synaptosomes, H_2O_2 generation induced by dopamine and 5-HT was MAO-dependent, MAO-A being the only source of H_2O_2 for 5-HT (Figure 2). Previous studies from our group established that MAO-dependent metabolism contributed to MDMA-induced mitochondrial neurotoxicity (Alves *et al.*, 2007; 2009). Although 5-HT has been shown to be metabolized *in vitro* both by MAO-A ($K_m = 178 \pm 2$ μM) and MAO-B ($K_m = 1170 \pm 432$ μM), metabolism by MAO-B is minimal in the presence of MAO-A (Shih *et al.*, 1999). However, MAO-B is fully effective in the absence of MAO-A, as when metabolism occurs inside 5-hydroxytryptaminergic nerves (Alves *et al.*, 2009). Thus, our results agree with previously published studies in which 5-HT metabolism is associated with MAO-A, while dopamine metabolism is both MAO-A- and MAO-B-dependent (Nagatsu, 2004).

MAO-catalysed dopamine metabolism has DOPAC as a final product. Here, DOPAC induced extensive H_2O_2 formation that may be involved in dopamine-associated MDMA neurotoxicity. Accordingly, DOPAC and its aldehyde precursor 3,4-dihydroxyphenylacetaldehyde were described as possible neurotoxic agents in MAO-associated oxidative damage (Burke *et al.*, 2003).

5-HT is readily oxidized and, simultaneously, acts as a ROS scavenger (Uemura *et al.*, 1980). The dimer 5,5′-dihydroxy-4,4′-bitryptamine is the major product of 5-HT auto-oxidation at physiological pH and temperature, being formed in the presence of H_2O_2 and peroxidase (Wrona and Dryhurst, 1988). In the presence of MAO-A inhibitor clorgyline, we observed lower H_2O_2 levels after exposure of synaptosomes to 5-HT, relative to that of control values, which can be explained by H_2O_2 consumption during the formation of 5-HT dimers in control conditions, as previously observed in cultured rat microglia (Huether *et al.*, 1997).

As demonstrated by several studies (Gollamudi *et al.*, 1989; Bai *et al.*, 1999; Esteban *et al.*, 2001), metabolism is required for MDMA neurotoxicity. Our results showed that MDMA metabolites, in mouse brain synaptosomes, induce a significant production of H_2O_2 in a concentration- and time-dependent manner, an effect that was not observed for the parent compound MDMA (Figure 1A–D). According to these results, MDMA metabolites exhibit higher neurotoxic potential than MDMA, as previously observed in rat cortical neurons (Capela *et al.*, 2006; 2007). Also, in other cell types, like rat cardiomyocytes (Carvalho *et al.*, 2004c), rat hepatocytes (Carvalho *et al.*, 2004b) and rat and human renal proximal tubular cells (Carvalho *et al.*, 2002), MDMA metabolites presented a higher toxic potential than the parent compound MDMA. Other reports indicate that peripheral metabolism of N-Me-α-MeDA and α-MeDA is required for neurotoxic events (Miller *et al.*, 1996). In fact, the conjugate 5-(GSH)-α-MeDA, which can be transported into the brain (Miller *et al.*, 1996), was the most potent H_2O_2 generator. Thus, our findings are consistent with previous studies, in which we demonstrated that conjugated metabolites of the catechols exhibited a higher neurotoxic potential in rat cortical neurons (Capela *et al.*, 2006; 2007).

The mechanism underling the toxicity of MDMA metabolites is thought to involve the inherent reactivity of their catechol moiety (Carvalho *et al.*, 2004b). MDMA metabolites α-MeDA, N-Me-α-MeDA and 5-(GSH)-α-MeDA, as well as dopamine, L-DOPA and DOPAC are prone to the oxidation to the corresponding *o*-quinones (Spencer *et al.*, 1998; Macedo *et al.*, 2007), which may further undergo redox cycling and generate the extensive H_2O_2 production observed in our studies. Therefore, antioxidants are expected to reduce not only *o*-quinones-related injury, but also the deleterious effects mediated by ROS and RNS. Accordingly, we observed that the antioxidants NAC, ascorbic acid and melatonin partially prevented the increase of H_2O_2 levels induced by MDMA metabolites α-MeDA, N-Me-α-MeDA and 5-(GSH)-α-MeDA, as well as by 5-HT, dopamine, L-DOPA and DOPAC (Figure 3).

ROS, being normal products of mitochondrial respiration (Adam-Vizi, 2005), are assumed to play a key role in the MDMA-related neurotoxicity (Cadet *et al.*, 1995;

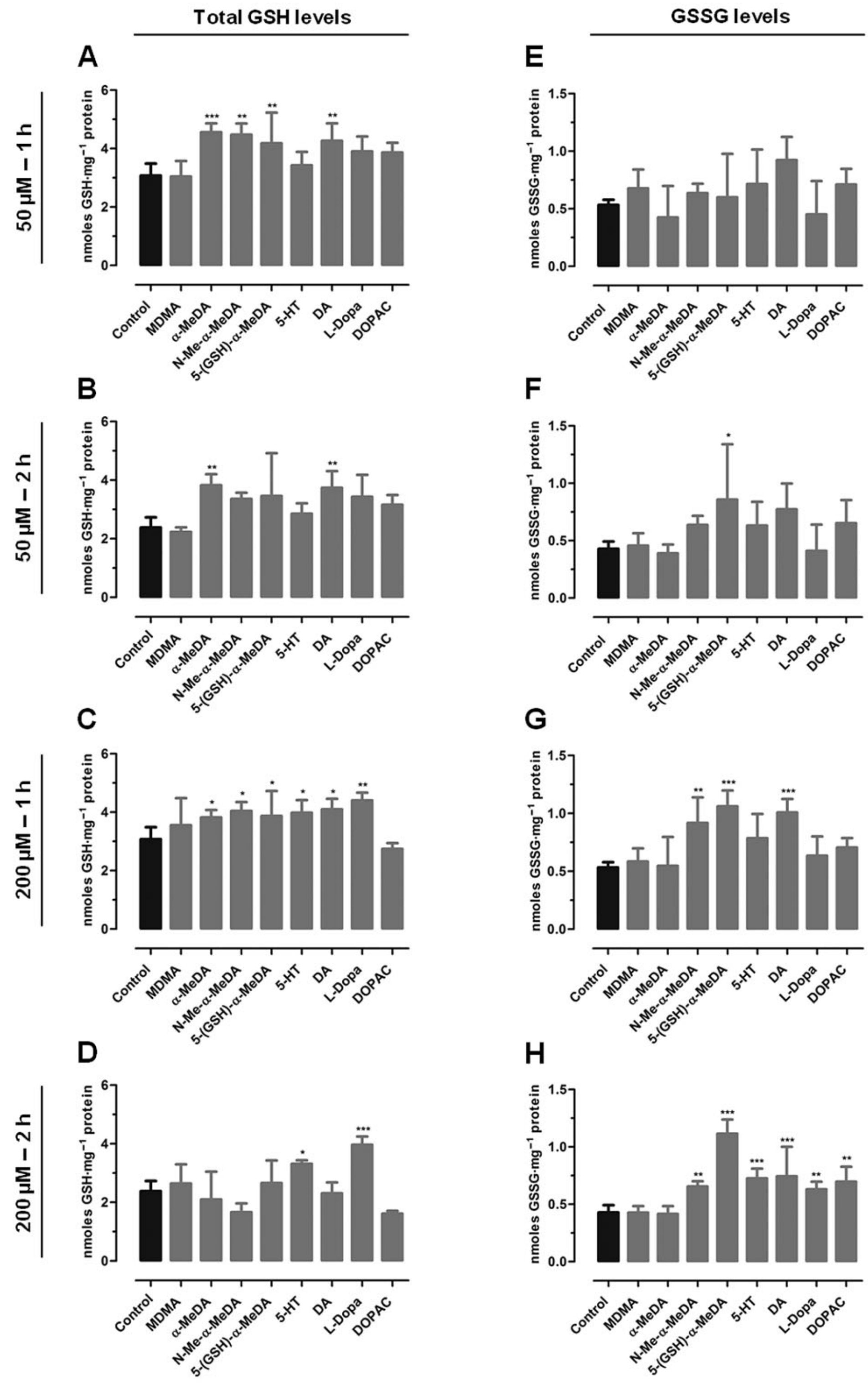

Figure 7

Effects of MDMA, its metabolites α-MeDA, N-Me-α-MeDA and 5-(GSH)-α-MeDA, as well as 5-HT, dopamine, L-DOPA and DOPAC, on total GSH and GSSG levels, in mouse brain synaptosomes, evaluated by the DTNB/GSH reductase recycling assay. Intra-synaptosomal total GSH (A, B, C and D) and GSSG levels (E, F, G and H) are presented. Synaptosomes were exposed to MDMA, its metabolites α-MeDA, N-Me-α-MeDA and 5-(GSH)-α-MeDA, as well as 5-HT, dopamine, L-DOPA and DOPAC, for 1 h (A, C, E and G) and 2 h (B, D, F and H), at the concentrations of 50 (A, B, E and F) and 200 µM (C, D, G and H). Results are presented as mean ± SD from 6 independent experiments, expressed in nmol GSH or GSSG·mg^{-1} protein. Statistical comparisons were made using one-way ANOVA followed by the Newman–Keuls multiple comparison *post hoc* test (**P* < 0.05, ***P* < 0.01, ****P* < 0.001 compound vs. control).

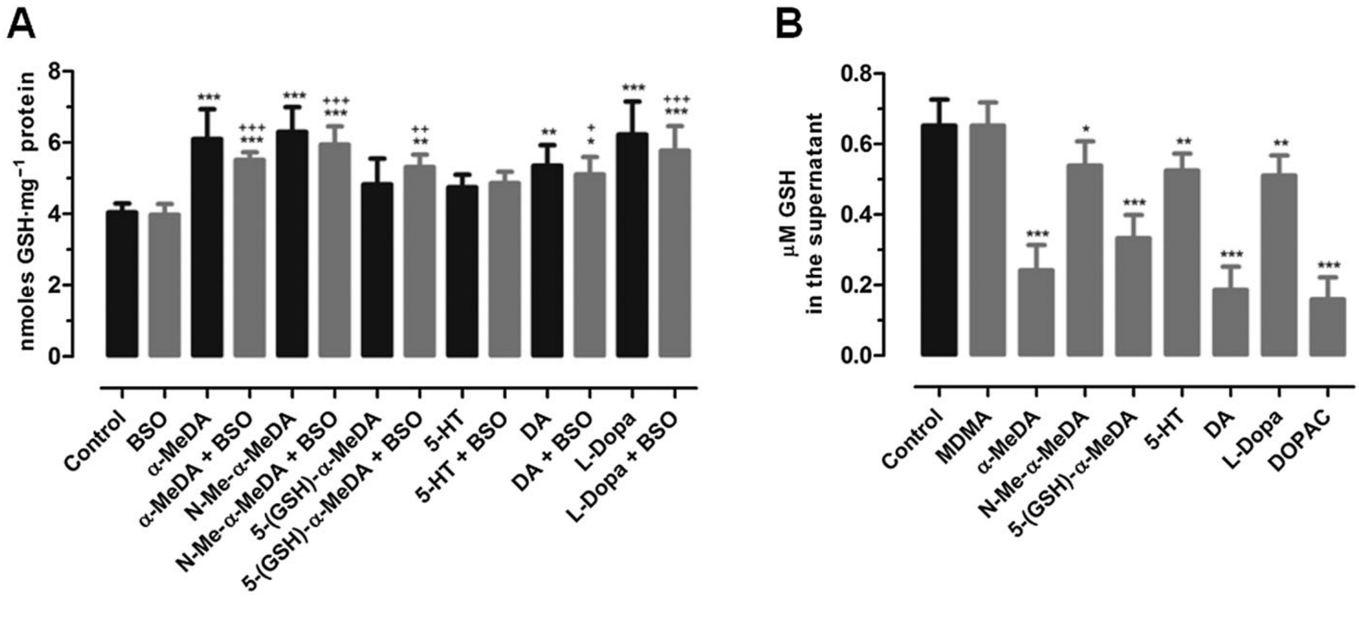

Figure 8

(A) Effect of pre-incubation with BSO (25 μM) on intra-synaptosomal total GSH levels elevation when synaptosomes were exposed to 200 μM of MDMA metabolites α-MeDA, N-Me-α-MeDA and 5-(GSH)-α-MeDA, as well as 5-HT, dopamine and L-DOPA for 1 h. (B) Total GSH levels in the supernatant after 1 h of incubation with 200 μM of MDMA, its metabolites α-MeDA, N-Me-α-MeDA and 5-(GSH)-α-MeDA, as well as 5-HT, dopamine, L-DOPA and DOPAC. Results are presented as mean ± SD from 6 independent experiments, expressed in nmol GSH·mg^{-1} protein (A) or μM GSH in the supernatant (B). Statistical comparisons were made using one-way ANOVA followed by the Newman–Keuls multiple comparison *post hoc* test (*$P < 0.05$, **$P < 0.01$, ***$P < 0.001$ treatment vs. control; $^{+}P < 0.05$, $^{++}P < 0.01$, $^{+++}P < 0.001$ compound + BSO vs. BSO).

Sanchez *et al.*, 2003). Although studies on isolated mitochondria have identified complex I and complex III as possible sites of ROS generation in the respiratory chain, complex I is likely to be a physiologically more relevant site (Votyakova and Reynolds, 2001). Therefore, interference with these mitochondrial complexes may increase ROS production. In this study, mitochondrial depolarization with the protonophore FCCP did not modify H_2O_2 generation induced by any of the tested compounds (Table 1). Although a recent *in vivo* study suggests that MDMA may inhibit mitochondrial complex I (Puerta *et al.*, 2010), the absence of effects in our experimental conditions is probably due to the fact that the whole brain synaptosome model lacks *in vivo* factors, like hyperthermia, inflammation, cell signalling and excitotoxicity.

MDMA can increase lipid peroxidation in the mouse striatum (Camarero *et al.*, 2002) and mitochondria from whole rat brain (Alves *et al.*, 2007; 2009). Though MAO-B strongly contributes to this effect *in vivo* (Alves *et al.*, 2007; 2009), in the present study, only the MDMA metabolite 5-(GSH)-α-MeDA significantly increased lipid peroxidation, in a concentration- and time-dependent manner (Figure 4A). It is noteworthy that during the preparation of synaptosomes, a significant proportion of brain mitochondria are lost, which may explain the absence of lipid peroxidation for 5-HT and dopamine, since MAO enzymes are located at the outer membrane of mitochondria. Lipid peroxidation induced by 5-(GSH)-α-MeDA was completely prevented by NAC (Figure 4B). Thus, the protective effect exerted by NAC on this process and in previous studies on MDMA metabolites (Capela *et al.*, 2006; 2007) suggests that this antioxidant may be an interesting drug to prevent MDMA-induced neurotoxicity.

MDMA metabolite-related *o*-quinones may arylate macromolecules and thus lead to gross structural and functional modifications including protein fragmentation, protein carbonylation, generation of protein peroxides and enzyme inactivation (Carvalho *et al.*, 2004a; 2004b; 2004c). In accordance, we found a significant increase in protein carbonylation, not only with the MDMA metabolite 5-(GSH)-α-MeDA, but also with DOPAC. Also, an increase in quinoprotein levels was observed when synaptosomes were exposed to the MDMA metabolites α-MeDA, N-Me-α-MeDA and 5-(GSH)-α-MeDA, as previously observed in rat cortical neurons (Capela *et al.*, 2007), as well as dopamine, L-DOPA and DOPAC, in a concentration-dependent but time-independent manner (Figure 5). The presence of the catechol group in these six compounds allows them to undergo redox cycling and the corresponding formation of *o*-quinones and subsequent binding to synaptosomal proteins. Likewise, the absence of the catechol group in the MDMA and 5-HT molecules explains the absence of increased quinoprotein levels for these compounds. Of note, the lower oxidation potential of these metabolites, when compared with the parent compound, correlated with a higher toxicity of these catechols to rat cortical neurons (Macedo *et al.*, 2007). Thus, the results herein shown for the H_2O_2 production, lipid peroxidation, quinoproteins

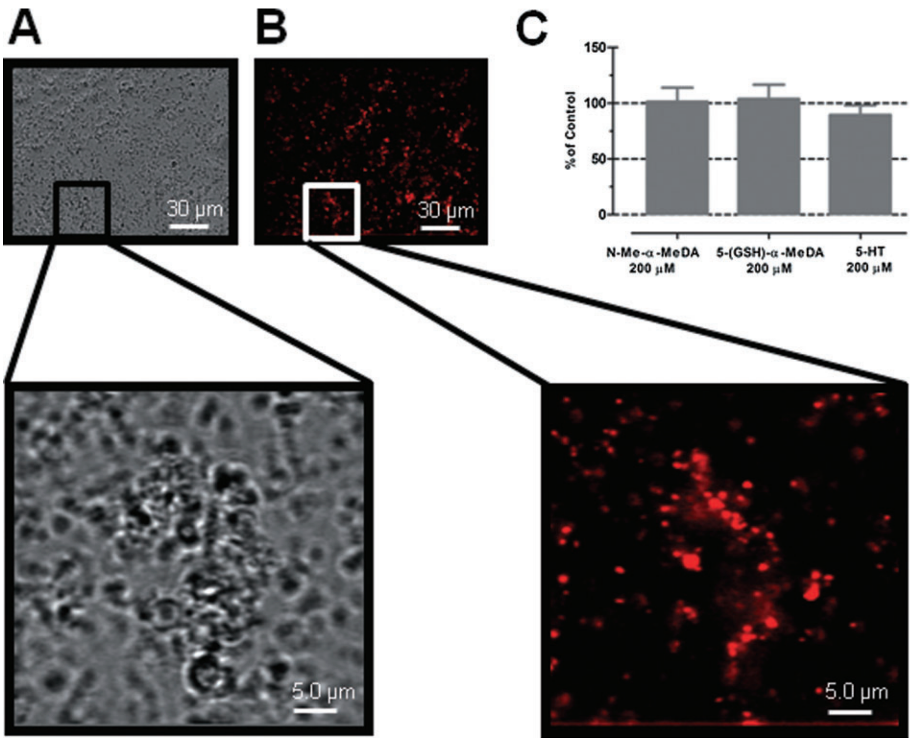

Figure 9

Microphotographs of control synaptosomes using bright field microscopy (A) and TMRM fluorescence (B) at 60× magnification. (C) Effects of MDMA metabolites N-Me-α-MeDA and 5-(GSH)-α-MeDA as well as 5-HT on the number of polarized mitochondria. Synaptosomes were exposed to 200 µM of MDMA metabolites N-Me-α-MeDA and 5-(GSH)-α-MeDA as well as 5-HT, for 1 h, then incubated with 50 nM TMRM and imaged as described under Methods during 2 h. Results are presented as mean ± SD from 6 independent experiments, expressed in percentage of control (number of polarized mitochondria per field, set to 100%). Statistical comparisons were made using one-way ANOVA followed by the Newman–Keuls multiple comparison *post hoc* test.

and protein carbonylation clearly demonstrate the high toxic potential of the MDMA metabolites, in particular 5-(GSH)-α-MeDA.

GSH, the most abundant intracellular antioxidant, plays a major role in protecting biological systems against oxidative stress. Incubation of synaptosomes with the tested compounds, except MDMA and its metabolite α-MeDA, significantly increased GSSG levels and decreased intra-synaptosomal total GSH levels from the first to the second hour of exposure, which can be a direct consequence of the pro-oxidant activity promoted by these compounds. However, as we previously reported, for the MDMA metabolites, decreased GSH levels may, as well, be due to GSH conjugation with reactive *o*-quinones and/or aminochromes produced during oxidation of these compounds (Carvalho *et al*., 2004c; Capela *et al*., 2007).

Administration of MDMA to rats causes oxidative stress in brain mitochondria (Alves *et al*., 2007; 2009). With this in mind, and considering that MAO is located at the outer membrane of mitochondria, we evaluated possible consequences of 5-HT (MAO substrate) and the MDMA metabolites N-Me-α-MeDA and 5-(GSH)-α-MeDA on mitochondrial integrity. As observed, in this experimental model, the oxidative stress mediated by 5-HT, N-Me-α-MeDA and 5-(GSH)-α-MeDA did not induce detectable mitochondrial dysfunction, as monitored by the average number of polarized mitochondria.

In conclusion, our study in mouse brain synaptosomes demonstrated that there was an increase in ROS generation associated with damage to cellular macromolecules promoted by MDMA metabolites. Moreover, the increase in monoamine neurotransmitters promoted by MDMA, namely 5-HT and dopamine, or their metabolites, such as DOPAC, can equally promote oxidative stress and contribute to MDMA neurotoxicity.

Acknowledgements

This work received financial support from 'Fundação para a Ciência e a Tecnologia (FCT)', Portugal (Project PTDC/SAU-FCF/102958/2008), under the frame of 'Programa Operacional Temático Factores de Competitividade (COMPTE) do Quadro Comunitário de Apoio III' and 'Fundo Comunitário Europeu (FEDER)'.

DJB, RS and JPC acknowledge 'Fundação para a Ciência e a Tecnologia' for their PhD grants (SFRH/BD/64939/2009 and SFRH/BD/29559/2006), and Post-doc grant (SFRH/BPD/30776/2006), respectively.

Silvana Araújo MSc, Vânia Vilas Boas MSc and Vera Marisa Costa PhD are gratefully acknowledged for their help in this work.

Conflict of interest

None.

References

Adam-Vizi V (2005). Production of reactive oxygen species in brain mitochondria: contribution by electron transport chain and non-electron transport chain sources. Antioxid Redox Signal 7: 1140–1149.

Alves E, Summavielle T, Alves CJ, Gomes-da-Silva J, Barata JC, Fernandes E *et al*. (2007). Monoamine oxidase-B mediates ecstasy-induced neurotoxic effects to adolescent rat brain mitochondria. J Neurosci 27: 10203–10210.

Alves E, Summavielle T, Alves CJ, Custódio JB, Fernandes E, Lourdes Bastos M *et al*. (2009). Ecstasy-induced oxidative stress to adolescent rat brain mitochondria in vivo: influence of monoamine oxidase type A. Addict Biol 14: 185–193.

Aubin N, Barneoud P, Carter C, Caille D, Sontag N, Marc C *et al*. (2004). SL25.1131 [3(S),3a(S)-3-methoxymethyl-7-[4,4,4-trifluorobutoxy]-3,3a,4,5-tetrahydro-1,3-oxazolo[3,4-a]quinolin-1-one], a new, reversible, and mixed inhibitor of monoamine oxidase-A and monoamine oxidase-B: biochemical and behavioral profile. J Pharmacol Exp Ther 310: 1171–1182.

Bai F, Lau SS, Monks TJ (1999). Glutathione and N-acetylcysteine conjugates of α-methyldopamine produce serotonergic neurotoxicity: possible role in methylenedioxyamphetamine-mediated neurotoxicity. Chem Res Toxicol 12: 1150–1157.

Bai F, Jones DC, Lau SS, Monks TJ (2001). Serotonergic neurotoxicity of 3,4-(±)-methylenedioxyamphetamine and 3,4-(±)-methylendioxymethamphetamine (ecstasy) is potentiated by inhibition of γ-glutamyl transpeptidase. Chem Res Toxicol 14: 863–870.

Burke WJ, Li SW, Williams EA, Nonneman R, Zahm DS (2003). 3,4-Dihydroxyphenylacetaldehyde is the toxic dopamine metabolite in vivo: implications for Parkinson's disease pathogenesis. Brain Res 989: 205–213.

Cadet JL, Ladenheim B, Hirata H, Rothman RB, Ali S, Carlson E *et al*. (1995). Superoxide radicals mediate the biochemical effects of methylenedioxymethamphetamine (MDMA): evidence from using CuZn-superoxide dismutase transgenic mice. Synapse 21: 169–176.

Cadet JL, Thiriet N, Jayanthi S (2001). Involvement of free radicals in MDMA-induced neurotoxicity in mice. Ann Med Interne 152: IS57–IS59.

Camarero J, Sanchez V, O'Shea E, Green AR, Colado MI (2002). Studies, using in vivo microdialysis, on the effect of the dopamine uptake inhibitor GBR 12909 on 3,4-methylenedioxymethamphetamine ('ecstasy')-induced dopamine release and free radical formation in the mouse striatum. J Neurochem 81: 961–972.

Capela JP, Meisel A, Abreu AR, Branco PS, Ferreira LM, Lobo AM *et al*. (2006). Neurotoxicity of ecstasy metabolites in rat cortical neurons, and influence of hyperthermia. J Pharmacol Exp Ther 316: 53–61.

Capela JP, Macedo C, Branco PS, Ferreira LM, Lobo AM, Fernandes E *et al*. (2007). Neurotoxicity mechanisms of thioether ecstasy metabolites. Neuroscience 146: 1743–1757.

Capela JP, Carmo H, Remião F, Bastos ML, Meisel A, Carvalho F (2009). Molecular and cellular mechanisms of ecstasy-induced neurotoxicity: an overview. Mol Neurobiol 39: 210–271.

Carvalho M, Hawksworth G, Milhazes N, Borges F, Monks TJ, Fernandes E *et al*. (2002). Role of metabolites in MDMA (ecstasy)-induced nephrotoxicity: an in vitro study using rat and human renal proximal tubular cells. Arch Toxicol 76: 581–588.

Carvalho M, Milhazes N, Remiao F, Borges F, Fernandes E, Amado F *et al*. (2004a). Hepatotoxicity of 3,4-methylenedioxyamphetamine and alpha-methyldopamine in isolated rat hepatocytes: formation of glutathione conjugates. Arch Toxicol 78: 16–24.

Carvalho M, Remiao F, Milhazes N, Borges F, Fernandes E, Carvalho F *et al*. (2004b). The toxicity of N-methyl-alpha-methyldopamine to freshly isolated rat hepatocytes is prevented by ascorbic acid and N-acetylcysteine. Toxicology 200: 193–203.

Carvalho M, Remião F, Milhazes N, Borges F, Fernandes E, Monteiro MC *et al*. (2004c). Metabolism is required for the expression of ecstasy-induced cardiotoxicity *in vitro*. Chem Res Toxicol 17: 623–632.

Carvalho M, Pontes H, Remião F, Bastos ML, Carvalho F (2010). Mechanisms underlying the hepatotoxic effects of ecstasy. Curr Pharm Biotechnol 11: 476–495.

Chipana C, Camarasa J, Pubill D, Escubedo E (2006). Protection against MDMA-induced dopaminergic neurotoxicity in mice by methyllycaconitine: involvement of nicotinic receptors. Neuropharmacology 51: 885–895.

Erecinska M, Nelson D, Silver IA (1996). Metabolic and energetic properties of isolated nerve ending particles (synaptosomes). Biochim Biophys Acta 1277: 13–34.

Erives GV, Lau SS, Monks TJ (2008). Accumulation of neurotoxic thioether metabolites of 3,4-(±)-methylenedioxymethamphetamine in rat brain. J Pharmacol Exp Ther 324: 284–291.

Esteban B, O'Shea E, Camarero J, Sanchez V, Green AR, Colado MI (2001). 3,4-Methylenedioxymethamphetamine induces monoamine release, but not toxicity, when administered centrally at a concentration occurring following a peripherally injected neurotoxic dose. Psychopharmacology 154: 251–260.

Gollamudi R, Ali SF, Lipe G, Newport G, Webb P, Lopez M *et al*. (1989). Influence of inducers and inhibitors on the metabolism in vitro and neurochemical effects in vivo of MDMA. Neurotoxicology 10: 455–466.

Granado N, O'Shea E, Bove J, Vila M, Colado MI, Moratalla R (2008). Persistent MDMA-induced dopaminergic neurotoxicity in the striatum and substantia nigra of mice. J Neurochem 107: 1102–1112.

Hiramatsu M, Kumagai Y, Unger SE, Cho AK (1990). Metabolism of methylenedioxymethamphetamine: formation of dihydroxymethamphetamine and a quinone identified as its glutathione adduct. J Pharmacol Exp Ther 254: 521–527.

Hrometz SL, Brown AW, Nichols DE, Sprague JE (2004). 3,4-Methylenedioxymethamphetamine (MDMA, ecstasy)-mediated production of hydrogen peroxide in an in vitro model: the role of dopamine, the serotonin-reuptake transporter, and monoamine oxidase-B. Neurosci Lett 367: 56–59.

Huether G, Fettkötter I, Keilhoff G, Wolf G (1997). Serotonin acts as a radical scavenger and is oxidized to a dimer during the respiratory burst of activated microglia. J Neurochem 69: 2096–2101.

Jones DC, Duvauchelle C, Ikegami A, Olsen CM, Lau SS, de la Torre R *et al*. (2005). Serotonergic neurotoxic metabolites of ecstasy identified in rat brain. J Pharmacol Exp Ther 313: 422–431.

Kim S, Westphalen R, Callahan B, Hatzidimitriou G, Yuan J, Ricaurte GA (2000). Toward development of an in vitro model of methamphetamine-induced dopamine nerve terminal toxicity. J Pharmacol Exp Ther 293: 625–633.

Lim HK, Foltz RL (1988). In vivo and in vitro metabolism of 3,4-(methylenedioxy)methamphetamine in the rat: identification of metabolites using an ion trap detector. Chem Res Toxicol 1: 370–378.

Lowry OH, Rosebrough NJ, Farr AL, Randall RJ (1951). Protein measurement with the folin phenol reagent. J Biol Chem 193: 265–275.

Macedo C, Branco PS, Ferreira LM, Lobo AM, Capela JP, Fernandes E *et al*. (2007). Sinthesis and cyclic voltammetry studies of3,4-methylenedioxymetamphetamine (MDMA) human metabolites. J Health Sci 53: 31–42.

Magalhães J, Ferreira R, Marques F, Olivera E, Soares J, Ascensão A (2007). Indoor climbing elicits plasma oxidative stress. Med Sci Sports Exerc 39: 955–963.

Miller RT, Lau SS, Monks TJ (1996). Effects of intracerebroventricular administration of 5-(glutathion-*S*-yl)-α-methyldopamine on brain dopamine, serotonin, and norepinephrine concentrations in male Sprague-Dawley rats. Chem Res Toxicol 9: 457–465.

Miller RT, Lau SS, Monks TJ (1997). 2,5-bis-(glutathion-*S*-yl)-[alpha]-methyldopamine, a putative metabolite of (±)-3,4-methylenedioxyamphetamine, decreases brain serotonin concentrations. Eur J Pharmacol 323: 173–180.

Nagatsu T (2004). Progress in monoamine oxidase (MAO) research in relation to genetic engineering. Neurotoxicology 25: 11–20.

Nicholls DG (1993). The glutamatergic nerve terminal. Eur J Biochem 212: 613–631.

Ninković M, Selaković V, Dukić M, Milosavljević P, Vasiljević I, Jovanović M *et al*. (2008). Oxidative stress in rat kidneys due to 3,4-methylenedioxymetamphetamine (ecstasy) toxicity. Nephrology 13: 33–37.

O'Hearn E, Battaglia G, De Souza EB, Kuhar MJ, Molliver ME (1988). Methylenedioxyamphetamine (MDA) and methylenedioxymethamphetamine (MDMA) cause selective ablation of serotonergic axon terminals in forebrain: immunocytochemical evidence for neurotoxicity. J Neurosci 8: 2788–2803.

Oliveira JMA, Gonçalves J (2009). *In situ* mitochondrial Ca^{2+} buffering differences of intact neurons and astrocytes from cortex and striatum. J Biol Chem 284: 5010–5020.

Pizarro N, Farre M, Pujadas M, Peiro AM, Roset PN, Joglar J *et al*. (2004). Stereochemical analysis of 3,4-methylenedioxymethamphetamine and its main metabolites in human samples including the catechol-type metabolite (3,4-dihydroxymethamphetamine). Drug Metab Dispos 32: 1001–1007.

Pubill D, Chipana C, Camins A, Pallàs M, Camarasa J, Escubedo E (2005). Free radical production induced by methamphetamine in rat striatal synaptosomes. Toxicol Appl Pharmacol 204: 57–68.

Puerta E, Hervias I, Goñi-Allo B, Zhang SF, Jordán J, Starkov AA *et al*. (2010). Methylenedioxymethamphetamine inhibits mitochondrial complex I activity in mice: a possible mechanism underlying neurotoxicity. Br J Pharmacol 160: 233–245.

Sanchez V, Camarero J, O'Shea E, Green AR, Colado MI (2003). Differential effect of dietary selenium on the long-term neurotoxicity induced by MDMA in mice and rats. Neuropharmacology 44: 449–461.

Shenouda SK, Carvalho F, Varner KJ (2010). The cardiovascular and cardiac actions of ecstasy and its metabolites. Curr Pharm Biotechnol 11: 470–475.

Shih JC, Grimsby J, Chen K (1999). Molecular biology of monoamine oxidase A and B: their role in the degradation of serotonin. In: Baumgarten HG, Gothert M (eds). Serotoninergic Neurons and 5-HT Receptors in the SNC. Springer: Berlim, pp. 655–670.

Spencer JPE, Jenner P, Daniel SE, Lees AJ, Marsden DC, Halliwell B (1998). Conjugates of catecholamines with cysteine and GSH in Parkinson's disease: possible mechanisms of formation involving reactive oxygen species. J Neurochem 71: 2112–2122.

Stone DM, Hanson GR, Gibb JW (1987). Differences in the central serotonergic effects of methylenedioxymethamphetamine (MDMA) in mice and rats. Neuropharmacology 26: 1657–1661.

de la Torre R, Farré M (2004). Neurotoxicity of MDMA (ecstasy): the limitations of scaling from animals to humans. Trends Pharmacol Sci 25: 505–508.

Tretter L, Adam-Vizi V (2007). Uncoupling is without an effect on the production of reactive oxygen species by *in situ* synaptic mitochondria. J Neurochem 103: 1864–1871.

Tretter L, Chinopoulos C, Adam-Vizi V (1998). Plasma Membrane Depolarization and Disturbed Na+Homeostasis induced by the Protonophore Carbonyl Cyanide-p-trifluoromethoxyphenyl-hydrazon in isolated Nerve Terminals. Mol Pharmacol 53: 734–741.

Uemura T, Shimazu T, Miura R, Yamano T (1980). NADPH-dependent melanin pigment formation from 5-hydroxyindolealkylamines by hepatic and cerebral microsomes. Biochem Biophys Res Commun 93: 1074–1081.

Votyakova TV, Reynolds IJ (2001). $\Delta\Psi$m-Dependent and -independent production of reactive oxygen species by rat brain mitochondria. J Neurochem 79: 266–277.

Whittaker VP (1993). Thirty years of synaptosome research. J Neurocytol 22: 735–742.

Wrona MZ, Dryhurst G (1988). Further insights into the oxidation chemistry of 5-hydroxytryptamine. J Pharm Sci 77: 911–917.

Youdim MBH, Gross A, Finberg JPM (2001). Rasagiline [N-propargyl-1R(+)-aminoindan], a selective and potent inhibitor of mitochondrial monoamine oxidase B. Br J Pharmacol 132: 500–506.

Zhou M, Diwu Z, Panchuk-Voloshina N, Haugland RP (1997). A stable nonfluorescent derivative of resorufin for the fluorometric determination of trace hydrogen peroxide: applications in detecting the activity of phagocyte NADPH oxidase and other oxidases. Anal Biochem 253: 162–168.